Noname manuscript No.
(will be inserted by the editor)

Statistics of particle accumulation in spatially developing turbulent boundary layers

G. Sardina · F. Picano · P. Schlatter · L. Brandt · C.M. Casciola

arXiv:1703.10433v1 [physics.flu-dyn] 30 Mar 2017

Received: date / Accepted: date

Abstract We present the results of a Direct Numerical Simulation of a particle-laden spatially developing turbulent boundary layer up to $Re_\theta = 2500$. Two main features differentiate the behavior of inertial particles in a zero-pressure-gradient turbulent boundary layer from the more commonly studied case of a parallel channel flow. The first is the variation along the streamwise direction of the local dimensionless parameters defining the fluid-particle interactions. The second is the coexistence of an irrotational free-stream and a near-wall rotational turbulent flow. As concerns the first issue, an inner and an outer Stokes number can be defined using inner and outer flow units. The inner Stokes number governs the near-wall behavior similarly to the case of channel flow. To understand the effect of a laminar-turbulent interface, we examine the behavior of particles initially released in the free stream and show that they present a distinct behavior with respect to those directly injected inside the boundary layer. A region of minimum concentration occurs inside the turbulent boundary layer at about one displacement thickness from the wall. Its formation is due to the competition between two transport mechanisms: a relatively slow turbulent diffusion towards the buffer layer and a fast turbophoretic drift towards the wall.

G. Sardina
Facoltà di Ingegneria, Architettura e Scienze Motorie,
UKE Università Kore di Enna, 94100 Enna, Italy
and Linné FLOW Centre, KTH Mechanics, SE-100 44 Stockholm, Sweden
E-mail: gaetano@mech.kth.se

F. Picano · P. Schlatter · L. Brandt
Linné FLOW Centre and SeRC (Swedish e-Science Research Centre)
KTH Mechanics, SE-100 44 Stockholm, Sweden

C. M. Casciola
Dipartimento di Ingegneria Meccanica e Aerospaziale, Sapienza University of Rome,
via Eudossiana 18, 00184 Rome, Italy

Keywords Inertial particles · Turbulent Boundary Layers · Wall flows · Turbophoresis · DNS

1 Introduction

The dispersion of a solid phase in turbulent wall-bounded flows occurs in many technological processes such particle-blade interactions in the turbines of aeronautical engines. Inertial particles transported in turbulent wall flows display a characteristic preferential accumulation close to the wall. This phenomenology is denoted turbophoresis [3,15] and has been the subject of research in the last three decades [1]. The turbophoretic drift towards the wall is essentially controlled by one nondimensional parameter, the viscous Stokes number, that is the ratio between the particle relaxation time $\tau_p = \rho_p\, d_p^2/(18\,\rho\,\nu)$ and the viscous time scale of the flow ν/U_τ^2, with ρ_p and d_p the particle density and diameter, ρ and ν the fluid density and viscosity, and U_τ the friction velocity. In particular, the strongest particle accumulation towards the wall is found when the Stokes number is about twenty five, $St^+ \sim 25$. Particles of vanishing Stokes number behave as passive tracers and are therefore uniformly distributed in a turbulent flow, whereas heavy particles become insensitive to the turbulence fluctuations, the ballistic limit at high Stokes numbers. A review of experimental studies and direct numerical simulation (DNS) of turbophoresis over the last years can be found in [21], with most recent simulations presented in [17,18]. In most of these previous investigations, the dynamics of the inertial particle has been studied in parallel flows such as channels or pipes [18,16,11, 8]. A different approach is necessary in spatially evolving flows where it is fundamental to understand the dynamics of the near-wall accumulation when the local Stokes number of the dispersed phase changes during the particle evolution, i.e. in the streamwise direction, leading to non trivial effects as those observed in particle-laden turbulent round jets [12]. In this context, we present here statistical data from a large-scale direct numerical simulations (DNS) of a spatially evolving particle-laden turbulent boundary layer at Reynolds number $Re_\theta = 2500$, based on the momentum thickness θ corresponding to a friction Reynolds number $Re_\tau = 800$ based on the friction velocity. This can be seen as a moderate Reynolds numbers in experiments but it is certainly high for a fully resolved numerical simulation [20]. The study of particle dynamics in spatial developing boundary layers assumes a fundamental role to advance our understanding in multiphase flows because it represents the most ideal flow where the Stokes number changes along the mean stream direction.

A nominal Stokes number $St_0 = \tau_p\, U_\infty/\delta_0^*$ can be defined to measure the amount of inertia of a single particle population by using the free-stream velocity U_∞ and the displacement thickness of the boundary layer at the inflow δ_0^* of the computational domain (or any reference station such as the seeding location). For a spatially evolving flow, more meaningful local Stokes numbers needs to be defined, both based on local internal units St^+, as usually defined

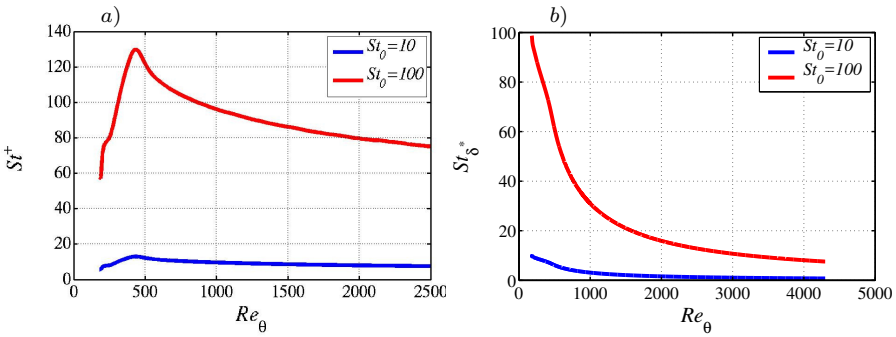

Fig. 1 *a*) Development of the viscous Stokes number St^+ in streamwise direction for two nominal Stokes numbers, St_0. *b*) Development of the external Stokes number St_{δ^*} in streamwise direction for two nominal Stokes numbers, St_0.

in parallel wall flows, and using external flow units St_{δ^*},

$$St^+ = \frac{\tau_p U_\tau^2}{\nu}, \qquad St_{\delta^*} = \frac{\tau_p U_\infty}{\delta^*}, \tag{1}$$

where it should be remarked that the displacement thickness of the boundary layer δ^* and the friction velocity U_τ change along the streamwise direction. Indeed, the two Stokes numbers decrease moving downstream in the boundary layer and tend to the limit of passive tracers. In figure 1 the two Stokes numbers are plotted versus Re_θ, the Reynolds number based on the momentum thickness θ, usually adopted to parametrize the streamwise distance in turbulent boundary layers [20]. As apparent by the decrease of the Stokes numbers, the effects of the inertia become less and less relevant in the downstream direction until the particles behave as fluid tracers at sufficient distance from the leading edge. Note that the decay rate is different for the two parameters, something discussed in further detail below. Both the inner and outer Stokes numbers are monotonically decreasing downstream when the boundary layer is fully turbulent; the peaks displayed by St^+ around $Re_\theta = 400$ occur in the region where the transition from laminar to turbulent state takes place.

Another peculiar aspect of the turbulent boundary layer is represented by the co-existence of two different zones, the inner turbulent region and the external free stream. These two regions are separated by an intermittent interface, the viscous super-layer [5], with a fractal nature where the enstrophy generated at the wall diffuses towards the outer irrotational free stream. In many applications, the particles usually lie in the outer region and then enter the turbulent inner region, crossing the separating interface.

This characteristic property, together with the spatial development of the turbulent boundary layer, introduces new features in the particle transport that cannot be investigated in parallel wall flows. In our recent study [19], we examined the same set of simulations and show that the concentration and

the streamwise velocity profiles are self-similar and depend only on the local value of the outer Stokes number and the rescaled wall-normal distance.

The aim of the present investigation is to further study the particle dynamics in a spatial boundary layer with emphasis on the distinction between particles that are seeded inside the turbulent regions and particles initially located outside the turbulent region, penetrating the shear layer and accumulating at the wall. In particular, we show that a minimum in the concentration profiles occurs at around one displacement thickness from the wall and this is the result of the competition of two transport mechanisms both directed towards the wall, but of different intensities. Particles are first subjected to a slow dispersion process from the outer region to the buffer layer and then to a fast turbophoretic drift close to the wall.

2 Numerical method

The numerical solver employed for the simulation is the pseudo-spectral code SIMSON [4]. The dimensions of the computational domain are $x_L \times y_L \times z_L = 3000\delta_0^* \times 100\delta_0^* \times 120\delta_0^*$ in the streamwise, wall-normal and spanwise directions with δ_0^* the displacement thickness at the inlet. The solution is expressed in terms of Fourier modes in the streamwise and spanwise direction with $n_x = 4096$ and $n_z = 384$, while $n_y = 301$ Chebyshev modes are used to discretize the wall-normal direction. Flow periodicity in the streamwise direction is handled with a fringe region at the end of the computational domain [10] where the velocity field is forced to the laminar Blasius profile at $Re_{\delta_0^*} = 400$. The flow is tripped just downstream of the inlet by a localized forcing random in time and in the spanwise direction to trigger the laminar-turbulent transition. To reach a fully developed turbulent flow, the carrier phase needs to reach a Reynolds number of the order $Re_\theta \simeq 1600$. In the present case, Re_θ varies from $Re_\theta \simeq 200$ at the inflow to $Re_\theta = 2500$ at the end of the computational domain. The unladen reference simulation is described in [20] where the same geometry and flow parameters are employed.

Regarding the dispersed phase, we assume that the particle concentration is dilute and neglect the backreaction on the flow, inter-particle collisions and hydrodynamic interactions among particles so that the one-way coupling approximation can be safely adopted. The particles are assumed to be small, rigid spheres with density one thousand times that of the carrier phase. The only force acting on the individual particle is the Stokes drag [9]. The fluid velocity at the particle position is evaluated by a fourth order spatial interpolation and the particle time integration is performed with a second order Adams-Bashforth scheme. Seven populations, differing only in the nominal Stokes number St_0, are evolved inside the computational domain. Particles are injected at a constant rate into the already turbulent flow at the streamwise location corresponding to $Re_\theta \simeq 800$ so that their evolution is not directly influenced by the trip forcing. For each population, particles are injected at the rate of 64 in δ_0^*/U_∞, randomly in the spanwise direction and at locations

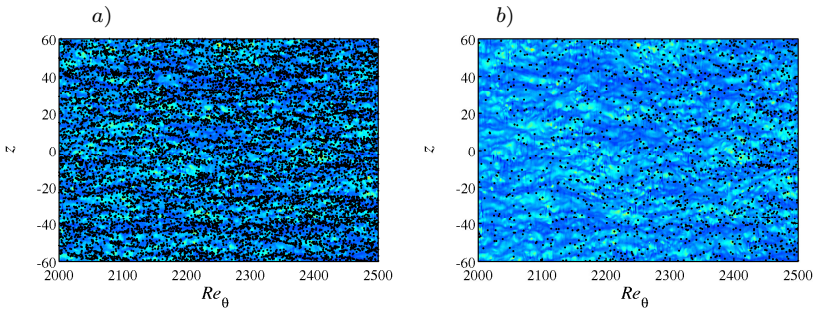

Fig. 2 Istantaneous configurations of inertial particles with nominal $St_0 = 30$ in the region close to the wall along a wall-parallel plane towards the end of the computational domain. Colours represent the values of the wall-shear stress (higher values lighter zones). *a*) Total particles in the given configuration. *b*) Particles initially released at a wall-normal distance larger than the local boundary layer thickness.

equispaced in the wall-normal direction in the range $y \in [0, 4\delta_{99}]$. Hence, a part of the total particles are released inside the turbulent region at a wall-normal distance below the boundary layer thickness δ_{99}, whereas the remaining particles are injected further away from the wall in the irrotational free stream. An example of a corresponding physical case is a flat plate moving with velocity $U_\infty = 5\, ms^{-1}$ in dusty air with particle diameters $d_p = 6 \div 60 \mu m$ and density ratio $\rho_p/\rho_f = 1000$. The computational domain describes the evolution of the particle-laden turbulent boundary layer until a momentum thickness $\theta = 5$mm. Computational time has been provided within the DEISA project WALLPART. Further details about the numerical simulation can be found in [19].

3 Results

3.1 Instantaneous visualizations

Two instantaneous configurations of the particle positions close to the wall are shown in figure 2 for the population with a nominal Stokes number $St_0 = 30$ in the region close to the end of the domain, i.e. with Re_θ ranging from 2000 to 2500. The background color represents the values of the local wall-shear stress τ_w, representative of the sweep/ejection events in the flow. In particular, it is known that high levels of wall-shear stress (lighter zones) correspond to a sweep event (fast velocity directed towards the wall) while the lower values (darker zones) are associated to the ejection events (slow velocity directed away from the wall) [13]. The visualization in figure 2*a*) displays the location of all particles, initially released both inside and outside the boundary layer. The particles tend to preferentially localize in regions of low wall-shear i.e. slow ejection events. This is consistent with the previous results from simulations in pipe and channel flows for the cases of most accumulating particles, $St^+ \sim 25$

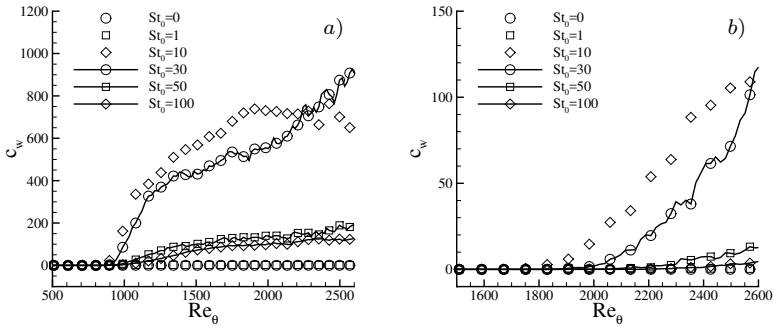

Fig. 3 Particle concentration close to the wall versus the streamwise coordinate indicated by Re_θ. *a*) Total particles inside the domain. *b*) Particles initially released outside the boundary layer thickness.

[21,11,18]. The viscous Stokes number of the population with nominal Stokes number $St_0 = 30$ decreases from $St^+ = 24$ at $Re_\theta = 2000$ to $St^+ = 22$ at $Re_\theta = 2500$ in the region depicted in the figure. As observed for parallel wall-bounded flows, the particles tend to stay in elongated streaky structures also in the spatial developing boundary layer, although this behavior appears to be less accentuated. This difference can be explained by the higher value of the friction Reynolds number $Re_\tau \simeq 700$ in the present case, to be compared with $Re_\tau \simeq 150 - 180$ of the typical channel flow simulations such as those analyzed in References [16,14,21,18].

The particles displayed in figure 2*b*) are all initially released outside the geometrical thickness of the boundary layer, δ_{99}. At $Re_\theta = 2000$ relatively few of these particles have reached the wall although their concentration at the wall increases monotonically when moving downstream along the domain. At the beginning of the accumulation phase particles do not show a preferential localization in the ejection events; only further downstream when a clear peak in the near-wall concentration profiles is forming, particles start to preferentially sample the low ejection events (low local wall-shear stress region). This observation is consistent with the dynamics of the spatial evolution of the turbophoresis discussed previously for pipe and channel flows [11,17]. At statistical steady state, particles accumulate in regions of vertical fluid motions away from the wall to compensate for the turbophoretic drift towards the wall, yielding in this way a zero net flux.

3.2 Particle concentration

The spatial evolution of the near-wall accumulation is reported in figure 3. Fig. 3*a* shows the wall concentration along the streamwise position identified by Re_θ. The wall concentration has been defined as the number of particles per unit volume found below a distance of $0.01\delta_0^*$ from the wall. The transient

accumulation phase is characterized by a strong particle drift towards the wall, i.e. turbophoresis, proportional to the local slope of the concentration profiles. This accumulation phase ends at a different streamwise distance according to the particle inertia and in general between $Re_\theta = 1100 \div 1500$. The particle populations characterized by a nominal Stokes number of 10 and 30 exhibit the highest turbophoretic drift. This phenomenon can be explained considering that the viscous Stokes number of these particles, $St^+ = 8 \div 30$, lies in the range of maximum turbophoresis when $Re_\theta = 1100 \div 1500$.

After this phase, we observe a secondary growth, characterized by a less steep slope. All the populations with $St_0 > 10$ remain in this second accumulation phase until the end of the computational domain, where particles with intermediate values of the relaxation time assume the highest wall concentration. At the end of this secondary phase, a peak in the concentration is reached only by particles with $St_0 = 10$, at the streamwise location corresponding to $Re_\theta \simeq 2200$; downstream of the maximum this population shows a slight decrease of the wall concentration. We expect a peak in the concentration for all the population once the local Stokes number becomes of order 20; however, this would happen at a larger distance from the computational inlet and an even longer computational domain would be required to capture this effect, something computationally too expensive for such kind of simulations. Theoretically, in an infinitely long streamwise domain all the particle populations will reach a concentration peak after the second accumulation phase, with the peak position dependent on particle inertia. This phenomenon can be explained considering that around $St^+ =\sim 25$ the turbophoresis is maximum and that in a turbulent boundary layer St^+ is always diminishing with the streamwise distance, i.e. Re_θ. Downstream of the location of maximum accumulation, the wall concentration will diminish since particles tend to the Lagrangian limit as their viscous Stokes number still decreases.

The near-wall accumulation of particles initially seeded outside the turbulent shear layer is displayed in figure 3*b*). The concentration increases monotonically for the most accumulating particle families and the behavior is similar to the phase of transient accumulation described in the discussion of the previous plot. The accumulation process starts at $Re_\theta = 2000$ and continues until the end of the computational domain. Also in this case the most accumulating particles are those characterized by the intermediate nominal Stokes numbers $St_0 = 10, 30$. Note that a clear peak for the near-wall accumulation cannot yet be distinguished in this case: the initial seeding has an effect on the maximum concentration and on the local values of the Stokes number where this maximum occurs, as the peak in concentration is reduced and moved further downstream when particles are seeded outside the boundary layer.

Figure 4 shows the wall-normal concentration profiles of different particle populations, St_0, at the three streamwise locations corresponding to $Re_\theta =$ 1500; 2000; 2500. On the left we show the statistics of all particles tracked in the simulation, whereas on the right we present results only for those initially released outside the turbulent boundary layer. Focusing on the left panels, the turbophoresis is apparent for the particles with $St_0 = 10 \div 100$ that exhibit

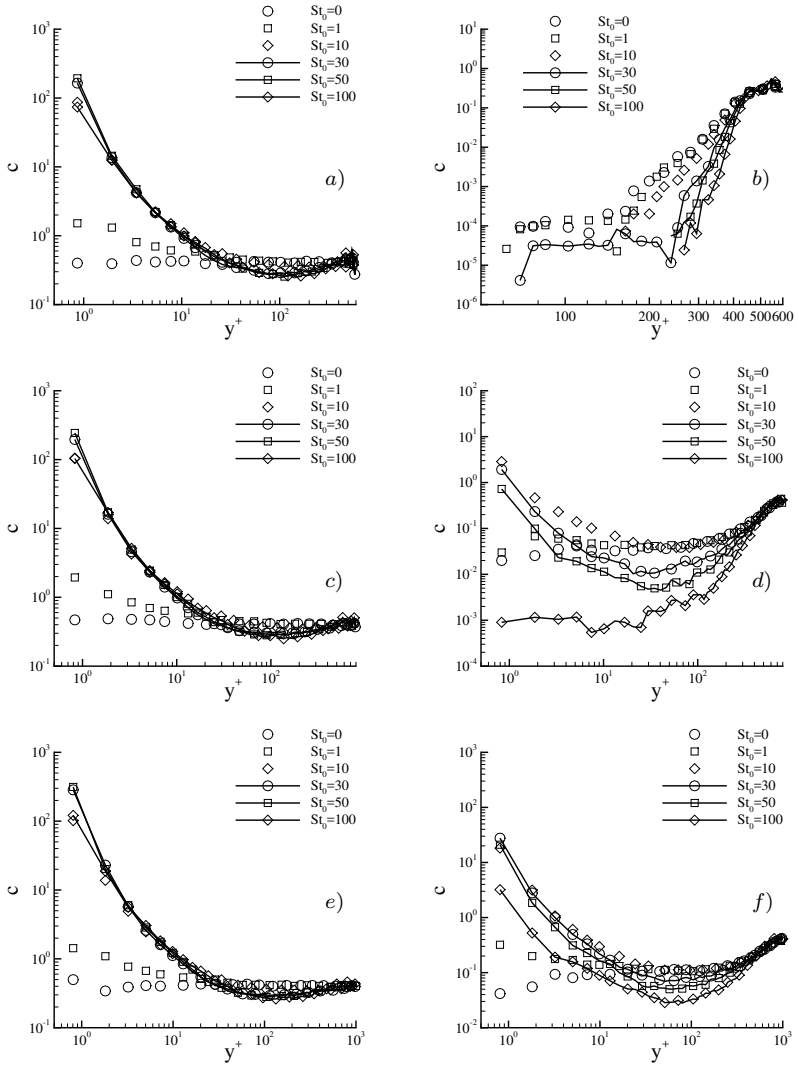

Fig. 4 Wall-normal profiles of the mean particle concentration in inner units y^+. Left panels: all particles inside the computational domain; right panels: particles initially released outside the boundary layer thickness. *a*), *b*) profiles at $Re_\theta = 1500$. *c*), *d*) profiles at $Re_\theta = 2000$. *e*), *f*) profiles at $Re_\theta = 2500$.

mean wall concentrations more than 100 times that of tracers, i.e. $St_0 = 0$, with no relevant differences when changing Re_θ. Particles of small inertia, $St_0 = 1$, do not show relevant turbophoresis, though still appreciable. Unlike the case of a turbulent channel flow, we see a minimum of the concentration for turbophoretic particles in the outer part of the boundary layer, $y^+ \approx 100$ in the figure, before the concentration recovers the unperturbed values further away

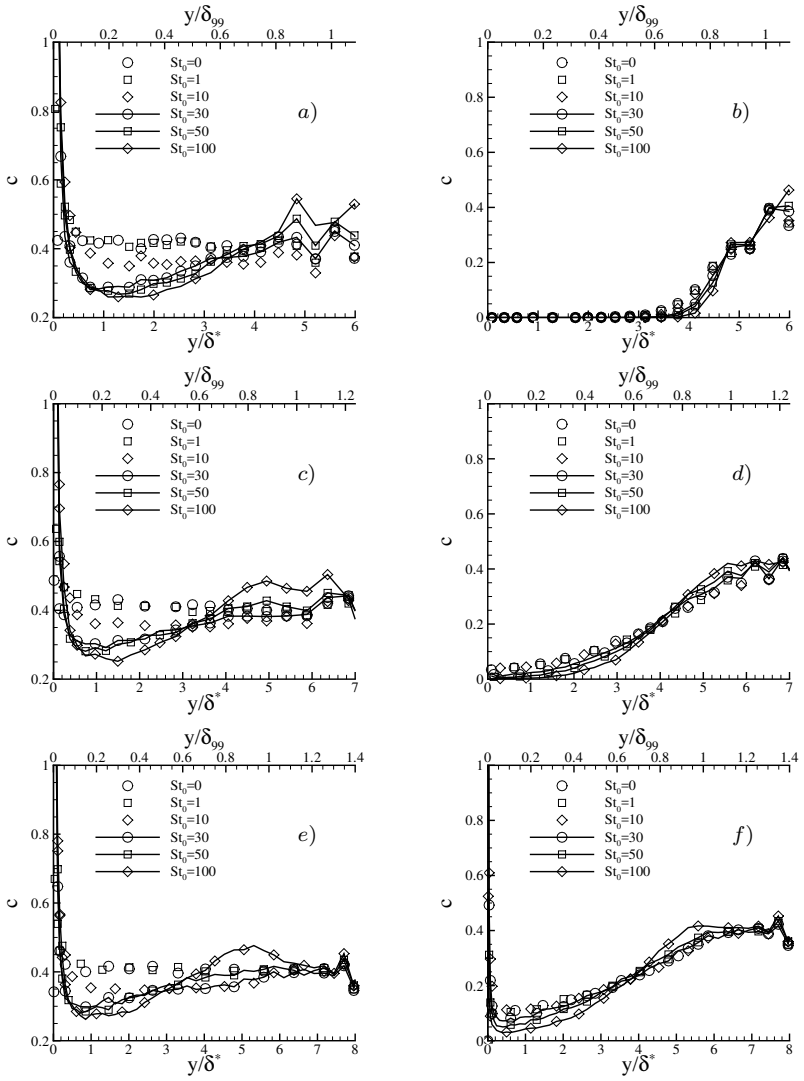

Fig. 5 Wall-normal profiles of the mean particle concentration in outer units, y/δ^* and y/δ_{99}. Left panels: all particles inside the domain; right panels: particles initially released outside the boundary layer thickness. *a*), *b*) profiles at $Re_\theta = 1500$. *c*), *d*) profiles at $Re_\theta = 2000$. *e*), *f*) profiles at $Re_\theta = 2500$.

from the wall. This minimum is originated by the combination of the strong turbophoretic drift that move the particles towards the wall and a gentler particle dispersion from the outer layer towards the bulk of the turbulent boundary layer. Indeed, the concentration profiles for the particles released in the external region of the boundary layer, plotted in the right panels of figure 4, show at the location corresponding to $Re_\theta = 1500$ that the particles

are still mainly concentrated in the outer region $y^+ > 300 \div 400$ and tend to slowly penetrate towards the wall; the near-wall concentration is however still negligible. The smaller the particle inertia the larger is the wall-normal turbulent diffusion that brings the particle from the external to the inner region. Moving downstream, $Re_\theta = 2500$, the turbophoretic drift becomes apparent from the near-wall peak close to the wall. Particles with $0 < St_0 \leq 50$ start to display values of concentration at the wall higher than those in the outer flow. This process leads to a concentration minimum in the outer part of the turbulent boundary layer that can be explained as follows. The particles reach the buffer layer by turbulent diffusion and are there accelerated towards the wall by the turbophoretic drift. This creates a region partially depleted of particles where the turbulent diffusion cannot compensate for the increased drift towards the wall provided by the turbophoresis.

The location of the minimum concentration scales in outer units, y/δ^*, as apparent from the left panels of figure 5. The concentration profiles show the minimum at $y \simeq \delta^*$ for all accumulating particles and Re_θ, while they become almost flat in the external free stream at $y > 5\delta^* \simeq \delta_{99}$. Particles initially released in the free stream, are shown in the right panels of figure 5. From the sequence in the figure one can recognize the initial uniform diffusion towards the wall, driven by the turbulent fluctuations, and finally the strong acceleration in the thin layer close to the wall, now driven by the turbophoresis, i.e. mainly by the particle inertia and their ability to filter high-frequency events.

The scaling of the minimum position in outer units, i.e. δ^*, highlights that the process is essentially controlled by the dynamics of the outer part of the boundary layer. As anticipated above, we argue that this minimum originates from the competition between the slower turbulent diffusion of the particles in the outer region of the turbulent boundary layer and the fast turbophoretic drift. From the right panels of figure 5, depicting the mean particle concentration in outer units for the particles initially released in the free stream, we see that the concentration is almost constant when $y > \delta_{99}$ and decreases towards the wall. Increasing Re_θ, i.e. moving downstream, the turbulent diffusion tends to increase the concentration inside the turbulent boundary layer. At $Re_\theta = 2500$, although the turbulent diffusion is still not able to evenly mix the particle inside the turbulent region, the turbophoresis is already apparent close to the wall, see the large concentration peak for $St_0 \geq 10$. These data indicate that the formation of the minimum in the concentration wall-normal profiles is due to an imbalance of the flux towards the wall driven by turbulence: a slow particle turbulent diffusion in the outer part of the turbulent boundary layer and a fast turbophoretic drift towards the wall.

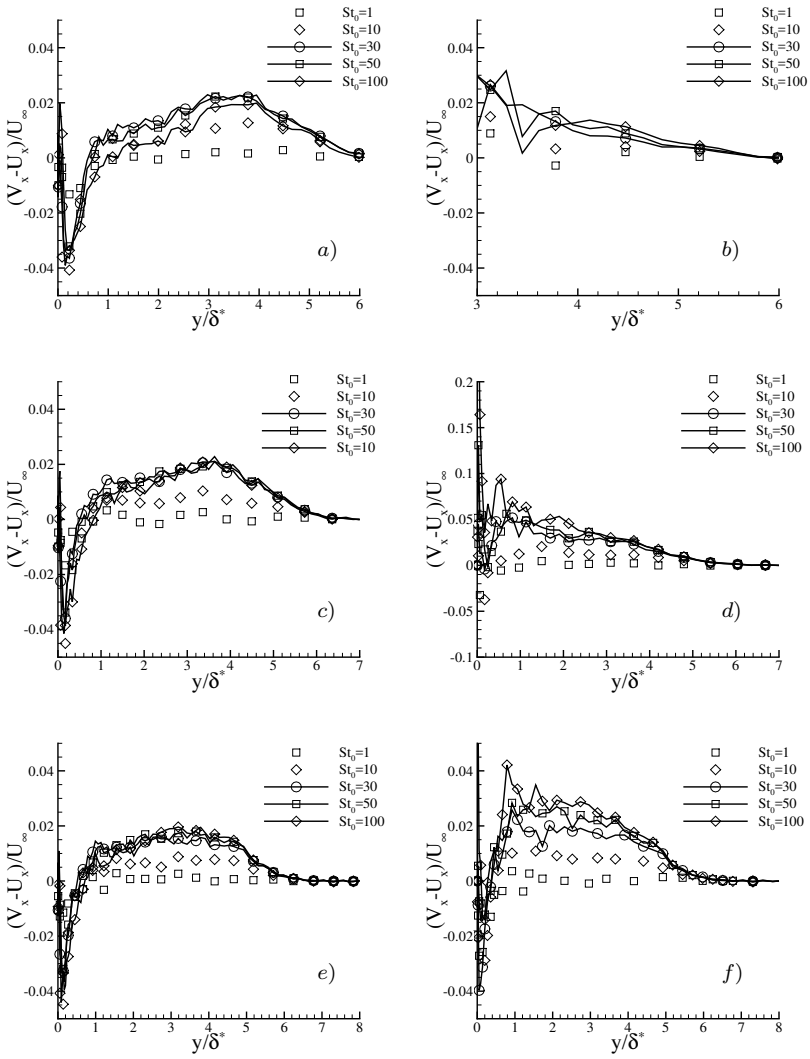

Fig. 6 Wall-normal profiles of the difference between the average streamwise particle velocity and the mean streamwise fluid velocity. Left panels: total particles inside the domain; right panels: particles initially released outside the boundary layer thickness. *a*), *b*) profiles at $Re_\theta = 1500$. *c*), *d*) profiles at $Re_\theta = 2000$. *e*), *f*) profiles at $Re_\theta = 2500$.

3.3 Particle velocity statistics

In order to analyze the differences between the fluid and particle motion, we report in figure 6 the difference between the mean particle streamwise velocity V_x and the mean streamvise fluid velocity U_x at three streamwise positions, *a*), *b*) at $Re_\theta = 1500$, *c*), *d*) at $Re_\theta = 2000$ and *e*), *f*) at $Re_\theta = 2500$, again for

all particles and for those seeded outside the boundary layer. We first consider the global particle behavior, independently of their initial injection point (left plots) and observe that all populations are faster than the mean flow in the outer region between $1 < y/\delta^* < 6$. Note that $y/\delta^* = 6$ roughly corresponds to the geometrical thickness of the boundary layer, δ_{99}. The position around $y/\delta^* = 1$, in correspondence with the minimum value of the concentration profile, is characterized by a mean particle streamwise velocity very close to that of the fluid. Hence this location, one displacement thickness from the wall, can be considered an equilibrium region for the particle dynamics. Below this point, in the region close to the wall, particles tend to be slower than the carrier phase. This is linked with the preferential localization of the particles in the low-speed streaks close to the wall, as also shown from the instantaneous configurations in figure 4. Inertial particles tend to preferentially stay in the slow ejection regions that are characterized by a streamwise velocity smaller than the mean flow in the near-wall region as a typical feature of turbophoresis.

In contrast with the results for the particle concentration, the fluid-particle velocity differences do not change significantly moving downstream. Larger differences between the particle and fluid streamwise velocity emerge for the particles initially released outside the boundary layer as shown in the right panels of figure 6. The data in *b*) show the profiles at $Re_\theta = 1500$ where just few particles have entered the turbulent boundary layer. Here the particles tend to be faster than the fluid as observed for the unconditioned case reported in the figure 6*a*). Further downstream, $Re_\theta = 2000$, panel *d*), the particles coming from the outer stream and diffusing into the boundary layer are much faster than the fluid displaying values of the velocity difference almost twice as large as those pertaining the unconditioned case in panel *c*). Particles captured by the boundary layer and approaching the wall from the irrotational free stream are characterized by a strong wall-normal velocity directed towards the wall that is associated with a streamwise velocity larger than that of the carrier phase. In other words, particles are seen to enter the boundary-layer wake region via large-structures similar to the high-speed streaks of near-wall turbulence: higher streamwise velocity with wall-normal velocity towards the wall. A similar trend is observed at $Re_\theta = 2500$, panel *f*), even though the effect is now weakened because the memory of the initial seeding position tends to be lost as particles move along with the flow.

4 Final Remarks

We report statistics of the dynamics of inertial particles transported in a spatially developing turbulent boundary layer. The Reynolds number based on the momentum thickness Re_θ increases from 200 to 2500 for the computational domain of the present simulation.

A boundary layer flow presents two main features that differentiate the behavior of inertial particles from the more studied case of a parallel turbulent flow, e.g. in channels and pipes, and it is therefore a relevant test case

worth investigation. The first is the variation along the streamwise direction of the local dimensionless parameters defining the fluid-particle interactions. The second is the coexistence of an irrotational free-stream and a rotational near-wall turbulent flow.

The first effect has been considered in [19]. Two different Stokes numbers have been defined, one using inner flow units and the other with outer units. Since these two Stokes numbers exhibit different decay rates in the streamwise direction, we found a decoupled particle dynamics between the inner and the outer region of the boundary layer. Preferential near-wall particle accumulation is similar to that observed in turbulent channel flow, while different behaviour characterizes the outer region. Here the concentration and the streamwise velocity profiles were shown to be self-similar and to depend only on the local value of the outer Stokes number and the rescaled wall-normal distance.

The scope of this paper is to examine the effect of the simultaneous presence of the external laminar stream and of the turbulent shear layer on the particle transport. In particular, we study how inertial particles released in the outer stream disperse inside the boundary layer and approach the wall. To this aim, we present statistics conditioned by the position of the initial injection and discuss the emergence of a minimum of the wall-normal particle concentration around the boundary layer thickness, $y \approx \delta^*$.

The imbalance between two different diffusion mechanisms, both directed towards the wall for particle coming from the free stream, induces the concentration minimum in the wall-normal direction. On one side, we have a relatively slow particle dispersion in the outer part of the boundary layer, due to the mixing by turbulent fluctuations, bringing the solid phase from the outer region to the buffer layer. On the other side, we have a fast turbophoretic drift due to the decrease of turbulent fluctuations closer to the wall pushing the particles towards the wall. The different magnitude of the two fluxes creates a region of lower concentration at the edge of the zones where each of the two mechanisms dominate.

The entrainment of particles in the turbulent regions is occurring in regions of higher streamwise velocity and wall-normal velocity towards the wall. Note that these structures, though similar to the near-wall high-speed streaks, are present across the laminar-turbulent interface at the boundary-layer edge effectively leading to a corrugated appearance of the instantaneous laminar-turbulent interface.

A similar minimum in concentration is not observed in channel flows where a laminar region acting as a reservoir of particles and imposing a reference external concentration, does not exist. Hence, there is no imbalance between the two fluxes mentioned above and the minimum concentration occurs at the channel midplane by symmetry.

The present results show that a non trivial dynamics occurs in intermittent regions, relevant for particle entrainment and mixing in several applications. Idealized shear-less configurations have been considered in [6,7] where both large fluctuations of the particle distribution and self-similar concentration

are observed. We expect that the presence of a mean shear in an intermittently turbulent/non-turbulent flow adds new interesting features as shown here for the entrainment of particles seeded in the laminar free stream. Using the configuration adopted here, we therefore plan to study the behavior of inertial particles in a transitional flow where turbulent spots appear randomly in space and time [2].

Acknowledgements The authors acknowledge DEISA (Distributed European Infrastructure for Supercomputing Applications) for the computer time granted within the project WALLPART. In particular, we thank EPCC (Edinburgh Parallel Computing Centre) for help in setting up the simulation and the assistance throughout the project. Resources at NSC (National Supercomputer Centre) at Linköping University, allocated via SNIC (Swedish National Infrastructure for Computing), were used for post-processing the data. We would like to acknowledge the support from the COST Action MP0806 *Particles in Turbulence*.

References

1. Balachandar, S., Eaton, J.K.: Turbulent dispersed multiphase flow. Ann. Rev. Fluid Mech. **42**, 447–464 (2010)
2. Brandt, L., Schlatter, P., Henningson, D.: Transition in boundary layers subject to free-stream turbulence. J. Fluid Mech. **517**, 167–198 (2004)
3. Caporaloni, M., Tampieri, F., Trombetti, F., Vittori, O.: Transfer of particles in nonisotropic air turbulence. J. Atmos. Sci. **32**(3), 565–568 (1975)
4. Chevalier, M., Schlatter, P., Lundbladh, A., Henningson, D.S.: Simson: A pseudo-spectral solver for incompressible boundary layer flows. Tech. Rep. TRITA-MEK 2007:07, KTH Mechanics (2007)
5. Corrsin, S., Kistler, A.: Free-stream boundaries of turbulent flows. Tech. rep., NACA (1955)
6. Gerashchenko, S., Good, G., Warhaft, Z.: Entrainment and mixing of water droplets across a shearless turbulent interface with and without gravitational effects. J. Fluid Mech. **668**, 293–303 (2011)
7. Ireland, P.J., Collins, L.R.: Direct numerical simulation of inertial particle entrainment in a shearless mixing layer. J. Fluid Mech. **704**, 301–332 (2012)
8. Marchioli, C., Soldati, A., Kuerten, J., Arcen, B., Taniere, A., Goldensoph, G., Squires, K., Cargnelutti, M., Portela, L.: Statistics of particle dispersion in direct numerical simulations of wall-bounded turbulence: Results of an international collaborative benchmark test. Int. J. Multiphase Flow **34**(9), 879–893 (2008)
9. Maxey, M.R., Riley, J.J.: Equation of motion for a small rigid sphere in a nonuniform flow. Phys. Fluids **26**, 883 (1983)
10. Nordström, J., Nordin, N., Henningson, D.: The fringe region technique and the fourier method used in the direct numerical simulation of spatially evolving viscous flows. SIAM J. Sci. Comput. **20**(4), 1365–1393 (1999)
11. Picano, F., Sardina, G., Casciola, C.: Spatial development of particle-laden turbulent pipe flow. Phys. Fluids **21**, 093,305 (2009)
12. Picano, F., Sardina, G., Gualtieri, P., Casciola, C.: Anomalous memory effects on transport of inertial particles in turbulent jets. Phys. Fluids **22**, 051,705 (2010)
13. Pope, S.: Turbulent Flows. Cambridge University Press (2000)
14. Portela, L., Cota, P., Oliemans, R.: Numerical study of the near-wall behaviour of particles in turbulent pipe flows. Powder Technology **125**(2), 149–157 (2002)
15. Reeks, M.: The transport of discrete particles in inhomogeneous turbulence. J. Aerosol Sci. **14**(6), 729–739 (1983)
16. Rouson, D., Eaton, J.: On the preferential concentration of solid particles in turbulent channel flow. J. Fluid Mech. **428**, 149–169 (2001)

17. Sardina, G., Picano, F., Schlatter, P., Brandt, L., Casciola, C.M.: Large scale accumulation patterns of inertial particles in wall-bounded turbulent flow. Flow Turb. Combust. **86**, 519–532 (2011)
18. Sardina, G., Schlatter, P., Brandt, L., Picano, F., Casciola, C.: Wall accumulation and spatial localization in particle-laden wall flows. J. Fluid Mech. **699**(1), 50–78 (2012)
19. Sardina, G., Schlatter, P., Picano, F., Casciola, C., Brandt, L., Henningson, D.: Self-similar transport of inertial particles in a turbulent boundary layer. J. Fluid Mech. **706**, 584–596 (2012)
20. Schlatter, P., Örlü, R., Li, Q., Brethouwer, G., Fransson, J.H.M., Johansson, A.V., Alfredsson, P.H., Henningson, D.S.: Turbulent boundary layers up to $Re_\theta = 2500$ studied through numerical simulation and experiments. Phys. Fluids **21**, 051,702 (2009)
21. Soldati, A., Marchioli, C.: Physics and modelling of turbulent particle deposition and entrainment: Review of a systematic study. Int. J. of Multiphase Flow **35**, 827–839 (2009)